Räisänen, V.I.; Alava, M.J.; Nieminen, R.M.

Fracture of three-dimensional fuse networks with quenched disorder

Published in:
Physical Review B

DOI:
10.1103/PhysRevB.58.14288

Published: 01/01/1998

Document Version
Publisher's PDF, also known as Version of record

Please cite the original version:
Räisänen, V. I., Alava, M. J., & Nieminen, R. M. (1998). Fracture of three-dimensional fuse networks with quenched disorder. *Physical Review B*, *58*(21), 14288-14295. https://doi.org/10.1103/PhysRevB.58.14288

Fracture of three-dimensional fuse networks with quenched disorder

V. I. Räisänen
ICA1, Universität Stuttgart, Pfaffenwaldring 27, D-70569 Stuttgart, Germany

M. J. Alava
Laboratory of Physics, Helsinki University of Technology, Otakaari 1M, Espoo, P.O. Box 1100, HUT-02015, Finland and NORDITA, Blegdamsvej 17, DK-2100 Copenhagen Ø, Denmark

R. M. Nieminen
Laboratory of Physics, Helsinki University of Technology, Otakaari 1M, Espoo, P.O. Box 1100, HUT-02015, Finland
(Received 12 January 1998; revised manuscript received 10 July 1998)

We study a fracture on a quasistatic time scale in a three-dimensional (3D) fuse network model with ''strong'' and ''weak'' disorder. These two cases differ noticeably in the development of the fracture. For strong disorder the damage scaling is very close to volumelike [number of broken bonds $N_b \sim L^3/(\ln L)^{0.3}$] unlike for weak disorder [$N_b \sim L^{2.4}/(\ln L)^{0.3}$]. With strong disorder global load sharing is only approximately valid. The size distribution of ''avalanches'' of broken fuses in the failure follows roughly a power-law scaling. The power-law exponent τ has a value close to 2, close to but differing from the exponent $-5/2$ expected of global load sharing. For weak disorder τ is about 1.5 which means that the decay of the size distribution is much slower than expected. These exponent values that characterize the development of damage prior to catastrophic failure are comparable to experimental ones. For the final fracture surfaces we observe a roughness exponent $\zeta \approx 0.4$ for weak disorder. For strong disorder, severe finite size effects are seen, but the exponent seems to converge to the same value as for weak disorder, which is close to the one for the 3D random bond Ising domain wall universality class. [S0163-1829(98)03642-X]

I. INTRODUCTION

In this work we study crack formation and roughness in disordered, three-dimensional (3D) brittle solids under conditions that correspond to slow crack growth. Slow growth implies that the crack advances in such a way that the stress fields always remain in equilibrium. The question of how disorder affects failure has recently become popular since the realization that crack surfaces allow for *a posteriori* conclusions about the failure process. In particular, the observed self-affine character of interfaces in fracture problems and the possibility of connections to fracture toughness[1] promise even practical engineering applications.

In the fractal range, fracture surfaces have been demonstrated to be self-affine over a range of length scales of several orders of magnitude. Hence the scaling of roughness r (standard deviation of the crack profile in the direction perpendicular to crack plane) can be written as $r \sim L^{\zeta}$. Both dynamics and the strength of disorder may affect the crack roughness scaling,[2] as measured by the roughness exponent ζ. One can also study the out-of-plane and in-plane exponents separately during failure.[3]

The question that remains is why the roughness exponent ζ attains its actual value. The experimental evidence at large enough length scales ($d \gg 1$ μm) exhibits a spectrum of results[4–8] centered around $\zeta = 0.8$, but does not seem to be universal, in contrast to early claims.[4] The high value of ζ makes it difficult to formulate a theory which would exhibit all the features that crack growth at large length scales and in driven, dynamic conditions shows.[9] At small scales and especially in the case of slow crack growth, such as, e.g., in fatigue or in the beginning of notched failure tests, it is believed that cracks are in general smoother—the variation of the surface in the perpendicular direction is smaller and ζ measured in that region has a lower value. In this case the role of dynamical effects such as crack bifurcation should be minimal. The observed roughness is small and one experimental exponent value is ≈ 0.45.[8] At nanometer scales crack roughness seems to be generally of the same order, e.g., for graphite[10] $\zeta = 0.43$. For soda-lime silicate glass, the large and small scale exponents are $\zeta = 0.87$ and $\zeta = 0.4$, respectively.[11]

Here we study adiabatic crack formation using the random fuse network (RFN) model in which the stress field has time to readjust completely after each microfracture. RFNs consist of individual fuse elements, which in the brittle case fail irreversibly when the local current exceeds a threshold value. They allow for a generic description of disorder in the material via the introduction of percolative disorder or local failure threshold distributions.

Two-dimensional RFNs have been studied extensively in the context of statistical mechanics of failure of brittle materials.[12] The breaking current I_b obeys for dilute lattices in 2D the system size (L) scaling $I_b/L \sim 1/\sqrt{\ln L}$,[13] and the same idea applies to the breaking potential V_b as well. With random breaking limits, the conclusion from numerical data is that $V_b/L \sim \text{const} + \mathcal{O}(1/L^2)$ for a brittle fracture in sufficiently large systems and $V_b/L \sim 1/(\ln L)^{0.8}$ for ''ductile'' fracture.[14] The concept of ductility means that despite the microscopic brittle fuse behavior the macroscopic response becomes smooth and the global conductivity does not exhibit a first order jump to zero from its macroscopic value in the precrack regime.

Damage, quantified by the total number of broken bonds N_b, can be divided to crack-related damage and off-crack path damage. For 2D systems the crack-related component would typically be expected to scale linearly with system size whereas the off-path damage may vary considerably. Kahng *et al.*[14] obtained $N_b \sim L + \text{const}$ for brittle disorder and $N_b \sim L^{1.6} + L$ for ductile fracture. de Arcangelis *et al.* have obtained scalings $N_b \sim L^{0.95-1.65}$ for various breaking limit distributions before the system enters the so-called catastrophic phase and $N_b \sim L^{1.71}$ for the total number of broken bonds.[15] The catastrophic phase is defined as the region of stress-strain curve beyond the maximum current along the *VI* curve. For the 3D case, the scaling laws of damage and failure current/voltage have been studied by Sahimi and Arbabi[16,17] with a qualitatively similar picture emerging as in 2D.

The generation of damage and the nature of the *VI* curve (analogous to the stress-strain curve) are related to the question as to what happens in the absence of a dominating crack. Once a propagating large crack has been formed it is natural to expect the propagation to become ''trivial,'' that is, the current needed to advance the crack should decrease. Also the scaling of the damage in this phase should arise from microfailures in the ''fracture process zone,'' an area around the crack tip. How this zone behaves during crack growth and in the presence of various kinds of disorder is nontrivial, the mechanics of self-affine cracks being not understood very well.[18] The question is whether the concept of a well-defined stress-intensity factor makes sense in the presence of fluctuations close to the crack tip.

In contrast, in the early stages of crack growth the microfailure dynamics should be controlled by statistics—the distribution of local failure limits—and by global load sharing since macroscopic crack growth is not dominant. It has recently been claimed by Hansen and Hemmer[19] and Zapperi *et al.*[20] that the 2D RFN can be mapped in a special (ductile) case to a global load sharing fiber bundle model. The observed ''avalanches'' or small-scale microfractures seem in that case to obey similar statistics as fiber bundle models with global load sharing, in which the process is exactly solvable by a mapping to a random walk with drift.[21] The energy release accompanied by such avalanches is in principle directly measurable with acoustic emission[22] and thus should make comparing theory and experiment possible.

The topology of cracks in RFN models has received little attention. Hansen, Hinrichsen, and Roux obtained a roughness exponent $\zeta \approx 0.7$ for various fuse failure threshold distributions for the 2D case.[23] The question of crack roughness in 2D and 3D has recently been reconsidered by Räisänen *et al.*, the conclusion being that the roughness exponent of 2D RFN failure interfaces seems to be very close to 2/3.[24] Thus 2D brittle failure is also in the directed polymer universality class, such as perfectly plastic yield interfaces,[25] for which ζ is via the KPZ equation known to be exactly 2/3.[26] Note that for 1+1D there is some experimental evidence that slow fracture surfaces scale with the expected exponent 2/3.[27] It is natural to ask whether the analogy can be extended to three dimensions. The 3D counterpart of a directed polymer is an Ising random bond domain wall. Numerical studies with graph theoretical optimization methods have reproduced the functional renormalization group prediction[28,29] $\zeta = 0.41 \pm 0.01$.

Here we analyze the failure of the 3D random fuse networks both from the point of view of fracture dynamics, and from the point of view of final fracture surfaces. The existing few studies of three-dimensional lattice systems have concentrated either on generic size-scaling behavior in small systems[16,17] or on failure of two-component networks.[30] Our own data concerning the scaling of the surface roughness with system size have been published in brief form elsewhere.[24] The computational model used is defined in Sec. II. In Sec. III we discuss the development of cracks in three dimensions and present some analytical estimates. Next, in Sec. IV, we proceed by showing results about the scaling of crack surfaces and of the scaling of various thermodynamical quantities (damage, voltage/current to failure, etc.). Section V ends the paper with a discussion of the results.

II. NUMERICAL MODEL

We employ an electrical analog of fracture in three dimensions to study fracture processes, namely, the random fuse network in a cubic lattice. The external voltage is applied in the *x* direction, the lattice has periodic boundary conditions in the *y* direction and free ones in the *z* direction. It is known that failure is more easily initiated near free boundaries.[31] This effect is caused by large surface currents. Hence the choice of boundary conditions affects, e.g., the scaling of roughness in different lateral directions, as will be seen in Sec. IV. A domain decomposition parallel version of the conjugate gradient method employing the PVM message passing library[32] has been used when running the code on a Cray T3D parallel computer. We have also used a Cray C90 vector computer for smaller system sizes. The system sizes used range from a linear size of $L=4$ to $L=48$. The scaling of the CPU time is approximately $t_{\text{CPU}} \sim L^{5.6}$ for largest system sizes in the parallel version, due to overhead introduced by message passing between processors.

We use the constant probability distribution

$$P(i_c) = \begin{cases} \dfrac{1}{w}, & i_c \in \left[1 - \dfrac{w}{2}, 1 + \dfrac{w}{2}\right], \\ 0, & \text{otherwise} \end{cases}$$

for the failure thresholds i_c of individual fuses. The width of the distribution *w* plays the role of a *disorder control parameter*. From studies of 2D random breaking limit RFNs it is known that the phase diagram of fracture should have three generic regimes as a function of *w*. For very small values the failure is ''trivial'' with a single crack nucleation event being sufficient to bring about the fatal crack.[14] At larger values of *w*, there is a nucleation phase ending in catastrophic crack formation. For large enough systems this leads to a trivial size scaling for the damage ($N_b \simeq L$). With both a distribution extending down to zero ($w=2$) and at $w<2$ in small enough systems a ductile phase exists having a nontrivial size scaling in N_b. The same kind of argument can be expected to hold also in three dimensions (the trivial scaling being L^2, naturally), although it is unknown how exactly the

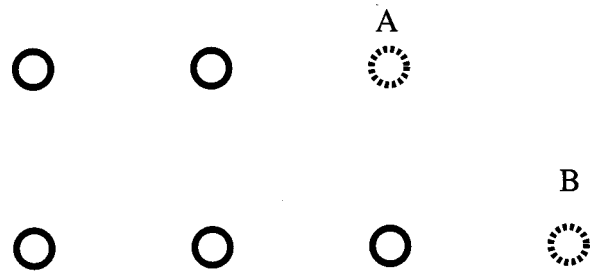

FIG. 1. The figure is a view of bonds in a cubic lattice perpendicular to the applied external voltage. The solid circles represent burnt fuses and those drawn in dashed line represent candidates of fuses to be burned next. In the fuse labeled A, the current enhancement is largest of all the neighboring fuses, 1.33, whereas, e.g., in B it is only 1.17.

lesser crack tip current enhancement and the larger number of neighboring potentially weak bonds balance each other as discussed in the next section.

III. GROWTH OF CRACKS IN 3D

A. Simple stability analysis

Fracture in two dimensions has usually been discussed using Lifshitz arguments, i.e., the concept of most critical defects.[13] The scaling properties of failure are then determined by the existence and formation of large defects for dilution-type disorder and failure threshold disorder, respectively. In two dimensions linear cracks are obvious candidate shapes, though the most critical defect geometry in 2D systems may be nontrivial.[33] The three-dimensional cubic lattice geometry allows for more complicated crack geometries than a planar square one. In 3D cubic lattices, the current enhancement near broken fuses is smaller than in 2D square lattices.[13] For neighbors of a single broken fuse we have $\alpha_{2D}=\pi/4\approx 1.273$ and $\alpha_{3D}\approx 1.093$. Therefore it can be expected that the amount of disorder required to cause a transition from a brittle fracture mode driven by local current enhancements to a ductile one is smaller in 3D. Another topological difference is that for an ensemble of ruptured fuses in an otherwise undamaged and homogeneous lattice, a round shape is preferred over a linear one (Fig. 1). This tendency can be viewed as a minimization of the interface of the crack area with intact fuses, or ''surface tension.'' This ''penny-shaped'' form is the most critical one in three dimensions, and has been used as a starting point in theoretical analyses in classical fracture mechanics.[34]

In the following, we present a three-dimensional version of the unstable crack analysis of Kahng *et al.* for 2D random breaking limit models.[14] One goal is to calculate the size-dependent limiting width w_c of the breaking limit distribution, below which the rupture mode is trivially brittle. Another aim is to try to obtain finite size scaling of the number of broken bonds required for the system to arrive at the catastrophic fracture phase N_c. The Kahng argument is based on the question: if a fuse fails, when does it automatically burn the nearest neighbor assuming that the current enhancement is the same as in the dilute damage limit?

In 3D there are roughly $3L^3$ fuses per system, and four neighbors in the lateral direction for each burnt fuse. The 3D current enhancement factor is $\alpha\approx 1.09$. The argumentation goes as follows. Let us denote with v_- (v_+) the lower (upper) bound of the breaking limit distribution, i.e., e.g., $v_-=1-w/2$. Let one assume that the breaking thresholds of single fuses are, on the average, evenly distributed in the range $[v_-,v_+]$. Then the breaking threshold of the nth weakest bond is given by

$$\langle v_{\text{weakest}}(n)\rangle = v_- + nw/L^3. \tag{1}$$

Notice that $v_->0$ makes the thermodynamic strength nonzero, unlike in cases with dilution disorder or a $P(i_c)$ extending down to zero. Similarly, one may deduce that the average threshold for the fuses surrounding the nth weakest one is given by

$$\langle v_{\text{edge}}(n)\rangle = v_- + w/(4n+1).$$

By equating $\alpha\langle v_{\text{weakest}}(n)\rangle$ and $\langle v_{\text{edge}}(n)\rangle$, one may deduce n, the number of fuses breaking as a consequence of current enhancement. For the case $w_c<w$ and $2-w\gg\mathcal{O}(1/L^{3/2})$ one may assume that the second term in Eq. (1) is negligible whereby the calculation gives for the damage N_c the finite, size-independent value

$$N_c(w<2)\approx\frac{w}{4v_-}\left[\frac{\alpha+1}{2(\alpha-1)}-\frac{1}{w}\right]. \tag{2}$$

For the strong disorder limit ($w\to 2$), the quantity $v_-\to 0$ and the result is

$$N_c(w=2)\approx L^{3/2}/\sqrt{2\alpha}. \tag{3}$$

The second approach is to ask how much failure can be accumulated in random, isolated fuse failures before these form cracks of size $a>1$. Burnings of fuses are considered to be independent, unless the fuses are adjacent in the direction perpendicular to the external voltage. For the number of statistically independent broken bonds N_{indep} one arrives with this assumption for $a=2$ at the result

$$N_{\text{indep}}\sim L^{3/2}. \tag{4}$$

The analysis hence results in a bound for the limiting width of the breaking limit distribution separating the brittle and ductile phases $w_c(L)\sim 2-\mathcal{O}(1/L^{3/2})$ as $L\to\infty$. The expectation is that the breaking mode is brittle (rapid crack growth) for disorder parameter values $w<2$ at the limit $L\to\infty$. Of course, the simplistic arguments are not complete: the stability argument is based on the assumption that the formation of larger cracks is immediately fatal and long-range interactions such as screening do not play any role. In Sec. III C we compare the predictions of the analysis presented here with the numerical data. We shall see that for the case of weak disorder they are valid up to the beginning of the catastrophic phase.

B. Formation of final cracks

Two examples of fracture surfaces are seen in Fig. 2 for low ($w=1$) and high ($w=2$) disorder. Diffuse damage—i.e., microfracture not belonging to the final fracture surface—is not shown. The $w=1$ case apparently corresponds to current enhancement controlled fracture for most

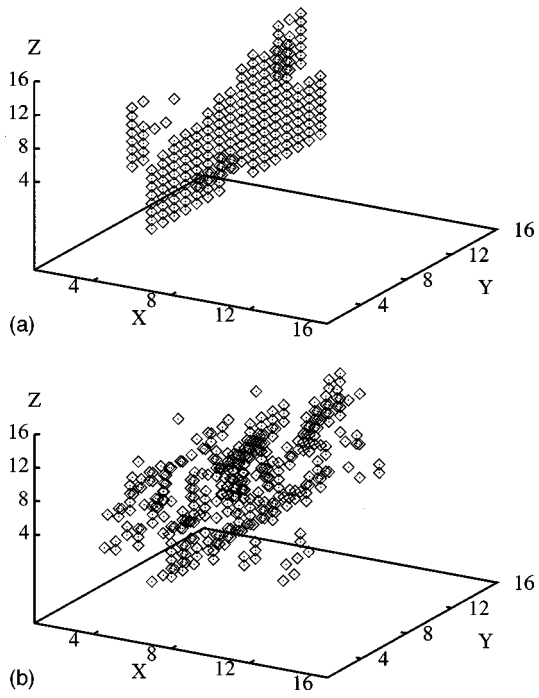

FIG. 2. Two examples of the fracture surfaces in a 3D random fuse network. Only broken fuses belonging to the final fracture surfaces are plotted. Left, $w=1$; right: $w=2$. System size is 16^3, and the total number of broken bonds in the $w=1$ case is 283 and in the $w=2$ case 2014.

of the process. In contrast, strong disorder dominates so that instead of a few major cracks the final fracture surface is formed out of a coalescence of a large number of microcracks. Note the total damage accumulated in both cases.

The onset of the catastrophic stage in the weak disorder case is characterized by strong localization of damage in the final fracture surface. The current enhancement created by the dominating large crack is sufficient to drive the crack further and overcome other competing cracks. A comparison of the weak and strong disorder cases is shown in Fig. 3, which displays the cumulative percentage of damage belonging to the macroscopic rupture zone. The percentage of burnt fuses belonging to the final fracture surface at any given moment can be viewed as an *order parameter*, a measure for the localization of the crack. The quantity plotted in Fig. 3 is an integral of this order parameter. The figure demonstrates that localization takes place for both values of w.

For weak disorder, the localization typically begins at the point where approximately 50% of the fuses eventually to be burnt have already done so and leads to around half of rupture events being centered in the fracture zone. For $w=2$, the (quite weak) localization takes place only after 80% of the eventual damage has taken place, except for $L=8$, where the localization seems to increase smoothly. For both weak and strong disorder, relatively large fractions of bonds belong to the final fracture surface. Based on this tendency showing up so frequently in both of the curves, quite often the final crack surface seems to be formed at the location where many of the first rupture events have taken place.

Next we study the fractions of burnt fuses belonging to the fracture surface y at the moment of macroscopic breakdown. The scaling of this quantity is approximately y

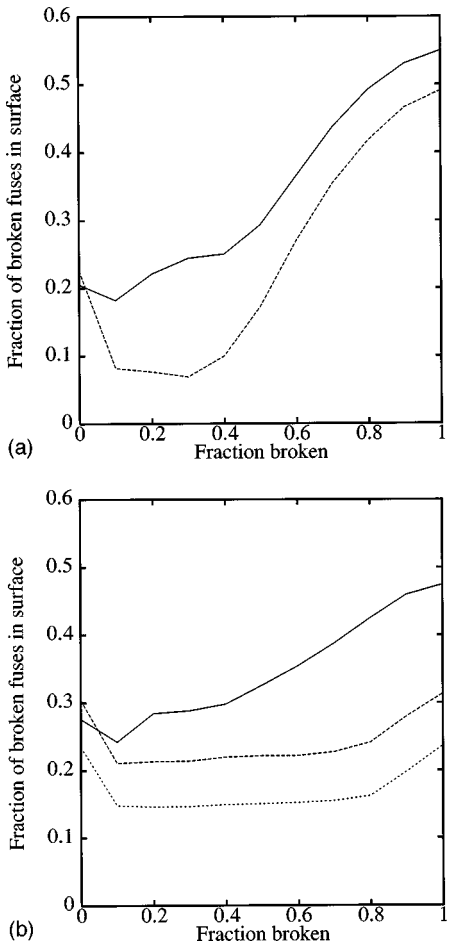

FIG. 3. Percentage of burnt fuses in the final fracture surface as a function of the number of broken bonds. The latter quantity has been scaled with the total number of broken bonds. Left, $w=1$ (solid line: $L=16$, dashed line: $L=40$); right, $w=2$ (solid line: $L=8$, dashed line: $L=16$, dotted line: $L=28$). Each of the curves is an average over five individual runs. Please note the different system sizes used in the two cases.

$\sim L^{-0.6}$ for strong disorder. If one assumes that the damage not belonging to the final fracture surface is almost percolationlike (say, scaling as $L^{3-\epsilon}$), one obtains an estimate for the fractal dimension D_f of the final fracture surface, namely,

$$y=\frac{L^{D_f}}{L^{3-\epsilon}}=L^{-0.6}, \tag{5}$$

from which one obtains $D_f=2.4-\epsilon$. It will be seen later that the scaling of the number of broken bonds is $L^{2.9}$ for $w=2$, which would yield $\epsilon=0.1$ and $D_f=2.3$. As discussed below, this is roughly in line with the roughness exponent obtained directly from the simulations. To summarize, Fig. 3 shows how for low disorder a single crack outperforms all the rivals and leads to current enhancement driven failure. With strong disorder, rupture proceeds with small cracks merging into larger ones all over the system.

C. Crack dynamics

Next we turn to the dynamics of fracture. Cumulative counts of burnt fuses as a function of external voltage (an

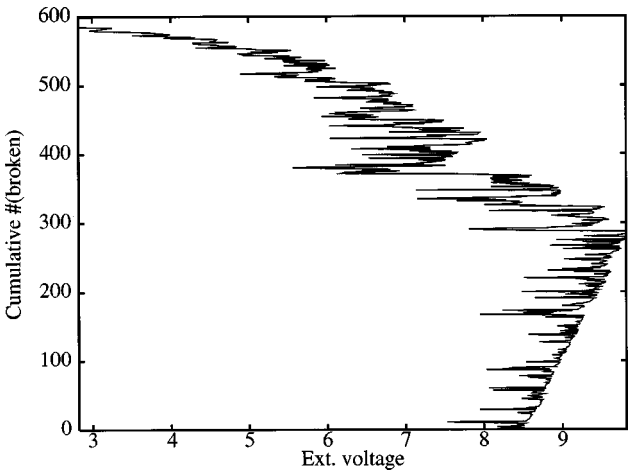

FIG. 4. Cumulative count of the burnt fuses as a function of the external voltage for $w=1$. Single simulation result; system size is 16^3.

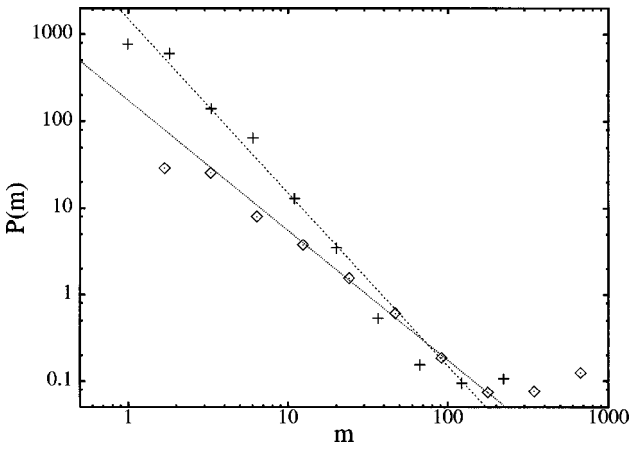

FIG. 5. Avalanche size distributions for $w=1$, $L=40$ (diamonds) and $w=2$, $L=28$ (+). Solid line: $\tau'=1.5$, dashed line: $\tau=2$. The lines are only guides to the eye.

example shown in Fig. 4) demonstrate that in the $w=1$ case a certain number of burnt fuses N_{cat} is required to bring the system to the catastrophic rupture regime after the first rupture event. This number is on the average close to 50% of the total number of broken bonds, a fact which is compatible with Fig. 3.

One of the central questions in the failure of fuse networks is when is the current enhancement close to microcracks important? Democratic load sharing fiber bundle models present a paradigm in which the local stress of an element is only dependent on the global damage, and thus the microscopic ''avalanches'' or microfracture events of several concurrently failing elements can be analyzed exactly.[21] For 2D fuse networks it has been shown recently that the global/democratic load sharing (GLS) principle may be applicable for strong disorder.[19,20] Questions still remain about the validity of the picture as fuse networks have size-dependent strength scaling laws.

The Zapperi *et al.* results[20] for the $w=2$ case show, similarly to the GLS fiber bundles, a power-law decay $n^{-5/2}$ ($\tau=5/2$) for the avalanche distribution (integrated over the whole fracture process as in the case of fiber bundles). Figure 5 shows the corresponding distribution for weak and strong disorder for our 3D RFN's for two large system sizes ($L=40$ for weak, $L=28$ for strong disorder). The data has been coarse grained by logarithmic binning into 10 bins for both cases. We find that the exponent (which should not be dimension dependent, if the GLS picture is correct) is roughly $\tau\approx 2.0$ for $w=2$, ignoring the high-end tail of the distribution. The tail exhibits strong fluctuations, and one should recall that the eventual failure of the mean-field model close to the point of catastrophic failure should be visible in exactly such a way. Note that one can study either current-driven or voltage-driven avalanches. In our case the exponent seems to be independent of the ensemble.

For $w=1$ the effective exponent is even smaller, $\tau\approx 1.5$. This would seem surprising, as larger cracks tend to be formed because of local stress enhancements. Thus one would expect a sharp decay of the avalanche distribution for large sizes as such ones would be equivalent to immediate catastrophic failure, and very rare. Simulations of fiber bundle models with local load sharing—failed fibers transfer their load to nearest neighbors—lead to much higher (but only effective) avalanche size exponents, $\tau>4$.[19,38] There is—at least to our knowledge—no theory that would be applicable to such precursor statistics with both global load sharing and local current enhancement effects. A future idea would be to consider the variation of τ with system size and the correlation lengths of avalanches with disorder. Both the exponents extracted from the avalanche statistics are of the same order as those measured by Garcimartin *et al.* for acoustic emission in mode I failure of 3D media.[22]

For the weak disorder case, the scaling of N_{cat} with system size is quite close to L^2 (Fig. 6). The prediction of Eqs. (3) and (4) for the ending of the noncorrelated phase appears to be too low for all system sizes simulated. The prediction given by the independent fuse burning picture for the rupture potential of the nth fuse, $v_n\approx v_- + nw/L^3$, holds quite well in 3D up to the catastrophic phase. The number of broken bonds as a function of voltage per fuse $n(v_n)$ grows in the simulations slightly faster than the prediction for $w=1$ and slightly slower than the one for $w=2$. This is an indication that current enhancement plays a smaller role in 3D than in 2D when disorder is weak and also shows the trivial fact that

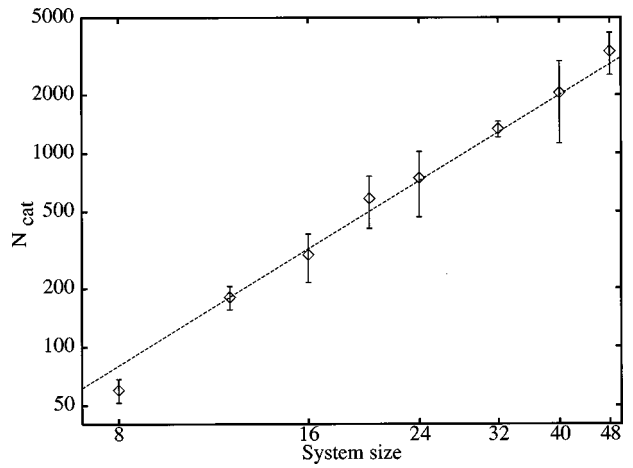

FIG. 6. Number of broken bonds before the catastrophic failure, for the weak disorder case. The line L^2 is only a guide to the eye.

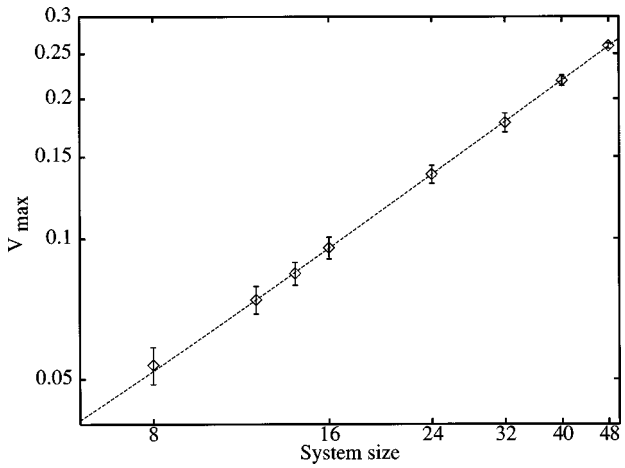

FIG. 7. The maximum voltage in the brittle case with the scaling $V_b/L \sim 1/(\ln L)^{0.3}$ shown with a line.

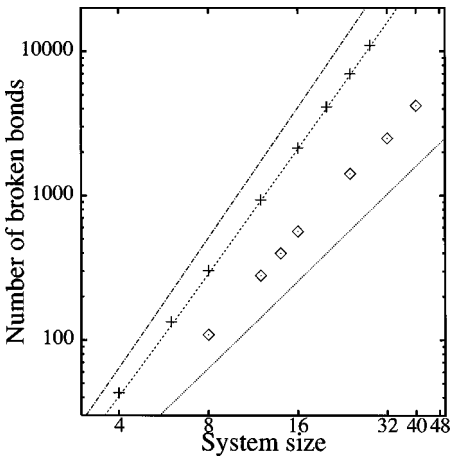

FIG. 8. The scaling of the total damage measured with average of the number of bonds broken during failure as a function of w. Upper dataset: $w=2$; lower one, $w=1$. The highest line indicates volumelike behavior ($\sim L^3$) and the lowest one the trivial limit ($\sim L^2$). The line drawn through $w=2$ data represents a $n_b \sim L^3/(\ln L)^{0.3}$ scaling.

the strong disorder case involves also stronger screening effects. Note that the picture of independent failure events is expected to be true only for the first part of the *VI* curve; the subsequent processes up to global failure are a different story.

In summary, the scaling of avalanche sizes in 3D appears to obey power laws but with smaller exponents than suggested previously on the basis of mean field-type global load sharing theory.[19,20] This result is in qualitative agreement with experimental evidence but cannot be explained with any of the known results from different models of load sharing in a system of elastic components in parallel. The approach based on the stability of cracks,[14] was found to give too low a value for finite size scaling of the beginning of the ''catastrophic'' phase of rupture. Before the catastrophic phase, not surprisingly, the assumption of uncorrelatedness of damage was found good.

IV. SCALING OF FRACTURE

A. Thermodynamical quantities

We discuss first the scaling of the breaking potential using the quantity $v_1 = V_1/L$, the voltage corresponding to the first fracture event in the system and $v_b = V_b/L$, the actual breaking potential of the system in relation to the voltage corresponding to the lower limit of the breaking limit distribution v_-. The Kahng-type argumentation for the breaking potential V_b predicts that the system is always brittle in the thermodynamic limit, if $w<2$. For both $w=1$ and $w=2$, the scaling can be fitted with the form $V_b \sim L/(\ln L)^{\gamma}$, with $\gamma = 0.3$ (Fig. 7). For strong disorder, this form applies for system sizes $L>10$. In the 2D case, a similar ansatz yields $\gamma \approx 0.8$,[14] and is applicable for strong disorder only. Sahimi and Arbabi find their force-displacement data $F(U)$ for three dimensions best collapsed with a trial function of the form[17] $F \sim [L^{\Omega_1}/(\ln L)^{\psi}]h(U/L^{\Omega_1})$, with $\psi = 0.2$, which is thus comparable to ours. The 3D numerical results correspond to the effective current enhancement being smaller than expected on analogy from two dimensions. The scaling of the maximum current which the system can sustain in both cases is approximately trivial, i.e., it is comparable to the cross-sectional area $L^{2.0}$.

The total number of broken bonds as a function of system size is close to a trivial fracture mode for $w=1$ [$N_b \sim L^{2.4}/(\ln L)^{0.3}$] and almost volumelike for $w=2$ (Fig. 8). The results for strong disorder are in particular consistent with a power-law scaling times a logarithmic correction, i.e.,

$$N_b \sim \frac{L^3}{(\ln L)^{0.3}}. \tag{6}$$

This is in accord with the scaling of the rupture potential, exactly as one would expect to be the case at the thermodynamical limit. The earlier 2D results for $w=0.7$–1.0 show a trivial scaling $N_b \sim L + \text{const}$ for $w=1.2$ and ''ductile'' one $N_b \sim L + L^{1.6}$ for $w=1.5$. The scaling of broken bonds in the limit of strong disorder agrees with the mean field picture that one gets by integrating $P(i_c)$ up to a L-dependent cutoff scale. The cutoff scale is consistent with a ''critical defect'' -type-like fracture point scaling. Straightforward power law fits $n_b \sim L^a$ result in the exponents $a=2.25$ and $a=2.95$ for weak and strong disorder, respectively. The logarithmic correction, however, seems to fit the data better and is consistent with the V_b scaling as well. Note finally the fact that n_b does not scale exactly with the system volume is also related to that the avalanche size exponent τ differs from the global load sharing one.

Finally we comment on the compatibility of the scaling of the number of broken bonds with that of V_b and I_b in the brittle case. In Sec. III C it was shown that the number of broken bonds before catastrophic failure scales approximately with the cross section of the system, $N_{\text{cat}} \sim L^2$. Since n_b increases faster with L this indicates that the damage accumulated in catastrophic crack propagation is nontrivial (faster than L^2).

B. Crack surface roughness

We measure the roughness of a rupture surface, possible overhangs excluded, using the ordinary definition, i.e., the average width of the interface

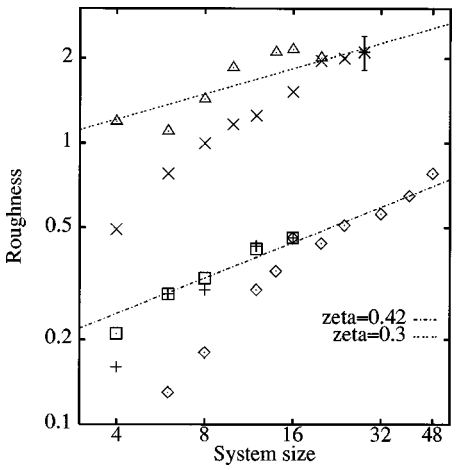

FIG. 9. Roughness of rupture interfaces [as defined in Eq. (7)] as a function of system size. Upper dataset: $w=2$, lower one: $w=1$. $\times$ and $\diamond$: raw data; $\triangle$, $+$, $\square$: sampling; upper dashed line: $\zeta=0.3$; lower dashed line: $\zeta=0.42$. The lines are only guides to the eye.

$$r=\sqrt{\langle h^2\rangle_{\mathbf{x}}-\langle h\rangle_{\mathbf{x}}^2}, \tag{7}$$

where $\langle\ \rangle_{\mathbf{x}}$ signifies averaging over spatial coordinates (here: perpendicular directions). The scaling of roughness as a function of the system size is measured with the exponent ζ, i.e., $r\sim L^{\zeta}$. A change in the exponent is seen at $w=1$ with small enough system sizes, which is most probably due to finite size effects. To correct for this, we compute ''windowed'' roughness, taking samples of size $L\times L$ of systems of size $M\times M$ with $M\geqslant 2L$. The sampling is performed in two ways, namely, by taking samples only of the middle of the system in the first case and averaging over many samples of each system in the second.

The results of this averaging are seen in Fig. 9, where it can be observed that the anomalous scaling of roughness at small system sizes disappears with the sampling method. For $w=2$, the ''raw'' data yield an exponent $\zeta\approx 0.7$ (in agreement with the D_f argument presented in Sec. III B), whereas the exponent obtained with sampling is consistent with minimum energy surface roughness. The difference between the two sampling techniques is due to boundary effects, a fact which will be illustrated below.

The distribution of roughness values $P(r)$ is not Gaussian, but has a tail extending towards large values. Hence normal symmetric error bars do not give a correct description of the variability of roughness. It turns out that with the sampling method, this asymmetry is amplified in the sense that when samples are taken from a larger system, the average roughness can be larger than the sample size. Of course, this does not occur in direct simulations. These undulations cause the averaged roughness of the samples to differ from the most frequent value of roughness in the $P_{\text{sampled}}(r)$.

To analyze the effect of anisotropic boundary conditions, we have measured the height-height correlations

$$C(l)=\sqrt{\langle[h(\mathbf{x})-h(\mathbf{x}')]^2\rangle_{\mathbf{x},\mathbf{x}'}},\quad |\mathbf{x}-\mathbf{x}'|=l \tag{8}$$

of the surface in both directions perpendicular to the external voltage. It can be shown[35] that $C(l)\sim l^{\zeta}$. The results display differences between the periodic and free directions, as could be expected. $C(l)$ for weak disorder data yields approximately 0.4 ± 0.1 for the scaling exponent of $C(l)$. The use of height-height correlation functions in measuring the value of the roughness exponent ζ at short distances [$\mathcal{O}(10)$] can be questioned, but $C(l)$ can be viewed as a means of possible differentiation between the two directions even if it does not give the value of ζ precisely.

The roughness results obtained by measuring directly the width of the rupture interface and calculating the height-height correlation functions show that the roughness exponent may be universal.[24] That is, ζ would attain its random bond Ising value of 0.41 after initial finite size crossover effects. According to the results of Hansen *et al.* the scaling of fracture quantities in two dimensions does not depend on the breaking threshold distribution, as long as there are no excessively strong bonds.[36] If very strong bonds exist, they can trap a propagating crack, given that their volume fraction is large enough. Assuming that the universality of the scaling of fracture quantities also applies to 3D, the possible universality of roughness exponents would extend also to distributions different from the constant one used by us. This would also be the expectation based on the analogy with directed polymers in random media. In that case, for the scaling exponents to differ from the usual ones, the energy distributions should, e.g., have anomalous tails for large values.

V. DISCUSSION

We have presented results for a three-dimensional random fuse network model concerning the effect of disorder on the brittle and ductile fracture modes. The rupture of the system has been studied for two values of the strength of disorder and several system sizes and compared with analytical arguments. Comparisons were also made with earlier numerical results.

The increasing concentration of damage in the final fracture crack for weak disorder indicates that fracture is governed by a small number of relatively large cracks. When disorder is strong, the final rupture surface is formed by an amalgam of a large number of ''microcracks.'' However, the ''avalanche'' distribution of microcrack sizes does not follow a mean field picture of global load sharing. The power-law exponent for strong disorder, for which one could expect such behavior, is distinctly different from the analytical[21] value 5/2, about 2. This, combined with the damage scaling exponent (effective exponent close to 3), shows most likely that even the dynamics of the strong disorder case is governed by stress-enhancement effects in the final stages of rupture. For weak disorder we obtain an effective exponent whose value is unexpectedly still lower, about 1.5. It would be interesting to try to relate the apparent load sharing with the failure statistics. This has been recently attempted for more realistic fiber bundle models. The net outcome seems to be that the failure probability of large systems seems to be determined at a mesoscopic length scale, but with democratic load sharing at that level.[37]

The smaller current enhancement causes the three-dimensional system to be ''less brittle'' than its 2D counterpart at the same disorder level. This effect shows in the scaling of the number of broken bonds being further from the trivial fracture in 3D than in 2D. Also, the brittle case yields

the scaling $V_b \sim L/(\ln L)^x$ for the breaking potential, with $x = 0.3$. This scaling applies also to the strong disorder data for system sizes $L > 10$. The macroscopic fracture points are reflected in the damage accumulated, in spite of the fact that the $w = 2$-case has arbitrarily weak fuses[36] and could perhaps be expected to result in an algebraic scaling.

Our numerical data show that the finite size of the system affects the roughness results, as expected. After all the attainable system sizes are limited indeed, to say nothing about ranges in which continuum mechanics would be valid. Thus the scalings of crack surfaces of random fuse networks should be considered with a grain of salt. Nevertheless there is evidence of algebraic roughness, with ζ being close to the minimum energy surface value 0.41. In comparing our results with experimental data, we note that no initial notch for initiation of crack growth was used in our simulations. In our case, the fracture nucleates from weak regions in the system. Finally, any analytical description of the actual dynamics of crack growth as well as a rigorous derivation for the roughness of fracture surfaces is still lacking both in two and three dimensions for slow, adiabatic crack growth processes.

ACKNOWLEDGMENTS

We thank the Edinburgh Parallel Computing Center (EPCC) and Center for Scientific Computing (CSC) in Otaniemi, Finland for generous computing resources. This work has been supported by the European Union TRACS scheme, the Technology Development Center of Finland (TEKES), the Academy of Finland, and by U.S. DOE Grant No. DE-FG02-090-ER45418. M.J.A. would like to thank Phil Duxbury for many entertaining discussions.

[1] B. B. Mandelbrot, D. E. Passoja, and A. J. Paullay, Nature (London) **308**, 721 (1984).
[2] J. Schmittbuhl, S. Roux, and Y. Berthaud, Europhys. Lett. **28**, 585 (1994).
[3] P. Daguier and E. Bouchaud, in *Fracture—Instability Dynamics, Scaling, and Ductile/Brittle Behaviour*, proceedings of the MRS Fall Symposium 1995, Session Q (Materials Research Society, Pittsburgh, 1996), pp. 343-354.
[4] E. Bouchaud, G. Lapasset, and J. Planès, Europhys. Lett. **13**, 73 (1990), and references therein.
[5] E. Bouchaud and J.-P. Bouchaud, Phys. Rev. B **50**, 17 752 (1994).
[6] K. J. Måløy, A. Hansen, E. L. Hinrichsen, and S. Roux, Phys. Rev. Lett. **68**, 213 (1992).
[7] V. Yu. Milman, R. Blumenfeld, N. A. Stelmashenko, and R. C. Ball, Phys. Rev. Lett. **71**, 204 (1993).
[8] E. Bouchaud and S. Navéos, J. Phys. I **5**, 547 (1995).
[9] P. Daguier, B. Nghiem, E. Bouchaud, and F. Creuzet, Phys. Rev. Lett. **78**, 1062 (1997).
[10] S. Miller and R. Reifenberger, J. Vac. Sci. Technol. B **10**, 1203 (1992).
[11] E. Guilloteau, H. Arribart, and F. Creuzet, in *Fracture—Instability Dynamics, Scaling, and Ductile/Brittle Behaviour* (Ref. 3), pp. 365–370.
[12] See, e.g., chapters by A. Hansen, P. Duxbury and L. de Arcangelis, in *Statistical Models for the Fracture of Disordered Media*, edited by H. J. Herrmann and S. Roux (North-Holland, Amsterdam, 1990).
[13] P. M. Duxbury, P. L. Leath, and P. D. Beale, Phys. Rev. B **36**, 367 (1987); P. M. Duxbury, P. D. Beale, and P. L. Leath, Phys. Rev. Lett. **57**, 1052 (1986).
[14] B. Kahng, G. G. Batrouni, S. Redner, L. de Arcangelis, and H. J. Herrmann, Phys. Rev. B **37**, 7625 (1988).
[15] L. de Arcangelis and H. J. Herrmann, Phys. Rev. B **39**, 2678 (1989).
[16] S. Arbabi and M. Sahimi, Phys. Rev. B **41**, 772 (1990).
[17] M. Sahimi and S. Arbabi, Phys. Rev. B **47**, 713 (1993).
[18] A. S. Balankin, Eng. Fract. Mech. **57**, 135 (1997).
[19] A. Hansen and P. C. Hemmer, Phys. Lett. A **184**, 394 (1994).
[20] S. Zapperi, P. Ray, H. E. Stanley, and A. Vespignani, Phys. Rev. Lett. **78**, 1408 (1997).
[21] P. C. Hemmer and A. Hansen, J. Appl. Mech. **59**, 909 (1992); M. Kloster, A. Hansen, and P. C. Hemmer, Phys. Rev. E **56**, 2615 (1997).
[22] A. Garcimartin, A. Guarino, L. Bellon, and S. Ciliberto, Phys. Rev. Lett. **79**, 3202 (1997).
[23] A. Hansen, E. L. Hinrichsen, and S. Roux, Phys. Rev. Lett. **66**, 2476 (1991).
[24] V. I. Räisänen, E. T. Seppälä, M. J. Alava, and P. M. Duxbury, Phys. Rev. Lett. **80**, 329 (1998).
[25] S. Roux and A. Hansen, J. Phys. II **2**, 1007 (1992).
[26] M. Kardar and Y.-C. Zhang, Phys. Rev. Lett. **58**, 2087 (1987); D. A. Huse and C. L. Henley, *ibid.* **54**, 2708 (1985).
[27] J. Kertesz, V. K. Horvath, and F. Weber, Fractals **1**, 67 (1993).
[28] A. A. Middleton, Phys. Rev. E **52**, R3337 (1995).
[29] M. J. Alava and P. M. Duxbury, Phys. Rev. B **54**, 14 990 (1996).
[30] P. M. Duxbury, P. D. Beale, and C. Moukarzel, Phys. Rev. B **51**, 3476 (1995); C. Moukarzel and P. M. Duxbury, J. Appl. Phys. **76**, 4086 (1994).
[31] Y. S. Li and P. M. Duxbury, Phys. Rev. B **36**, 5411 (1987).
[32] A. Geist *et al.* (unpublished).
[33] P. M. Duxbury, R. A. Guyer, and J. Machta, Phys. Rev. B **51**, 6711 (1995).
[34] M. F. Kanninen and C. H. Popelar, *Advanced Fracture Mechanics* (Oxford University Press, Oxford, UK, 1985).
[35] A.-L. Barabási and H. E. Stanley, *Fractal Concepts in Surface Growth* (Cambridge University Press, Cambridge, UK, 1995), p. 303.
[36] A. Hansen, E. L. Hinrichsen, and S. Roux, Phys. Rev. B **43**, 665 (1991).
[37] W. A. Curtin, Phys. Rev. Lett. **80**, 1445 (1998).
[38] S. D. Zhang and E. J. Ding, Phys. Lett. A **193**, 425 (1994).